Supramolecular Chemistry

DOI: 10.1002/anie.201411272

Non-Centrosymmetric Homochiral Supramolecular Polymers of Tetrahedral Subphthalocyanine Molecules**

Julia Guilleme, María J. Mayoral, Joaquín Calbo, Juan Aragó, Pedro M. Viruela, Enrique Ortí, Tomás Torres,* and David González-Rodríguez**

Abstract: *A combination of spectroscopy (UV/Vis absorption, emission, and circular dichroism), microscopy (AFM and TEM), and computational studies reveal the formation of non-centrosymmetric homochiral columnar subphthalocyanine assemblies. These assemblies form through a cooperative supramolecular polymerization process driven by hydrogen-bonding between amide groups, π–π stacking, and dipolar interactions between axial B–F bonds.*

As a result of their singular structure, the columnar stacking of tetrahedral-shaped molecules can provide materials with exclusive properties that cannot be obtained using common planar π-conjugated discotics.[1] First, these molecules may exhibit intrinsic chirality,[2] which may potentially lead to the formation of non-centrosymmetric stacks in which helical chirality evolves from the molecule itself[3] and not from chiral centers present in peripheral side chains.[4] Second, these molecules are often endowed with axial dipoles that may add up along the stacks resulting in the formation of polar nanostructures, an effect which may be exploited to uniaxially align the columns in an electric field[5] or for the development of polarized semiconducting films.[6] However, the supramolecular convex–concave polymerization of related bowl- or cone-shaped monomers is in itself a challenging task.[7] As a result of their 3D structure, most bowl- or cone-shaped monomers are obviously reluctant to aggregate in solution. Moreover, many bowl-shaped aromatic molecules, such as corannulane, sumanene, calixarene, or cyclotriveratrylene, undergo cone inversion,[8] which leads to depolarization and stack racemization.

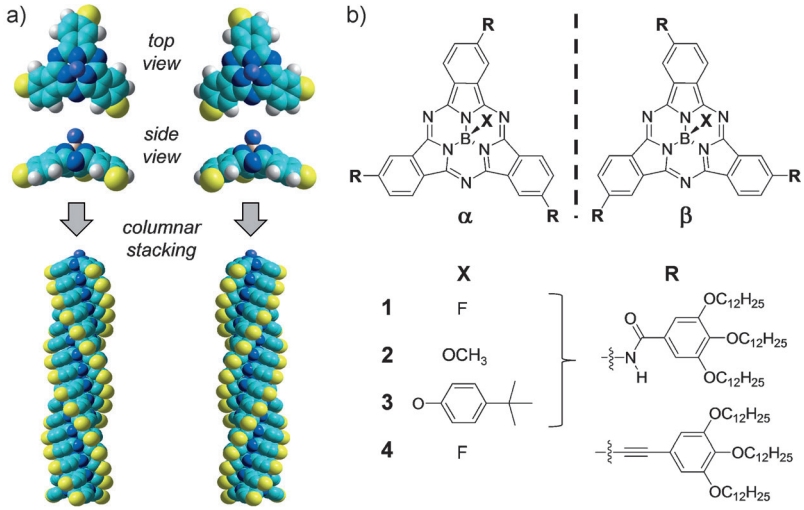

Figure 1. a) Top and side views of the two enantiomers of a model trisubstituted SubPcBF macrocycle and the corresponding homochiral head-to-tail columnar stacks. b) Molecular structures of the two enantiomers of compound **1** (**1α** and **1β**),[14,15] and compounds **2**, **3** and **4**. Atom colors in (a): N = blue, C = turquoise, H = white, and the yellow sphere represents a generalized R functional group.

Subphthalocyanines (SubPcs; Figure 1a)[9] are a rare example of π-conjugated aromatic molecules with a rigid tetrahedral structure.[10] They are composed of three isoindole units condensed around a boron atom which also bears an axial ligand perpendicular to the macrocyclic core. In contrast with their higher analogues the phthalocyanines (Pcs), whose supramolecular chemistry is dominated by π–π interactions between planar surfaces, SubPcs do not exhibit a strong tendency to aggregate in solution. This property, which stems from their nonplanar geometry, has proven beneficial for many applications in which dye aggregation needs to be prevented.[11] However, because of their intense absorption and emission in the visible region of the electromagnetic spectrum and their tunable electronic properties,[12] SubPcs have recently attracted significant technological interest in the fields of organic semiconductors and optoelectronics.[13]

[*] J. Guilleme, Dr. M. J. Mayoral, Prof. T. Torres, Dr. D. González-Rodríguez
Departamento de Química Orgánica, Facultad de Ciencias
Universidad Autónoma de Madrid, 28049 Madrid (Spain)
E-mail: tomas.torres@uam.es
david.gonzalez.rodriguez@uam.es
J. Calbo, Dr. J. Aragó, Dr. P. M. Viruela, Prof. E. Ortí
Instituto de Ciencia Molecular, Universidad de Valencia
46980 Paterna (Valencia) (Spain)
E-mail: enrique.orti@uv.es
Prof. T. Torres
IMDEA Nanociencia, Facultad de Ciencias
Cantoblanco, 28049 Madrid (Spain)

[**] Funding from MINECO (CTQ2011-24187, CTQ2011-23659, MAT2012-38538-CO3-01 and 02, FEDER funds CTQ2012-31914 and CTQ2012-35513-C02-01), CAM (S2013/MIT-2841 FOTO-CARBON), GVA (PROMETEO/2012/053 the European Research Council (StG-279548), and MECD (F.P.U. fellowships to J.G. and J.C.) is gratefully acknowledged.

Supporting information for this article is available on the WWW under http://dx.doi.org/10.1002/anie.201411272.

Such applications often demand suitable columnar organizations in which close π–π contacts contribute to efficient exciton and charge transport.[1]

Herein, we show for the first time that tetrahedral-shaped molecules such as SubPcs can be polymerized in solution to form self-assembled non-centrosymmetric homochiral columnar nanostructures. The key to overcome the challenging head-to-tail (convex–concave) stacking is the combination of hydrogen-bonding interactions between three peripheral amide groups and the use of an axial fluorine atom which provides minimal steric hindrance upon stacking[7c] and a strong axial dipole moment.

C_3-symmetric SubPcs **1**, **2**, **3**, and **4** (Figure 1b) were synthesized as racemic mixtures and characterized as described in the Supporting Information. The two enantiomers of **1**, hereafter called **1α** and **1β**, were then separated by analytical chiral HPLC (see Figure S1 in the Supporting Information) on a milligram scale.[15]

The first insights into the aggregation of enantiomers **1α** or **1β** in solution came from UV/Vis absorption and emission spectroscopy. In 1,4-dioxane, a competing solvent for hydrogen bonding, compounds **1α/β** display the characteristic narrow Q band features of monomeric SubPcs, that is, a maximum at $\lambda = 576$ nm ($\varepsilon = 86\,000\ \text{M}^{-1}\text{cm}^{-1}$) with shoulders at $\lambda = 530$ and 560 nm. In sharp contrast, **1α/β** solutions in methylcyclohexane (MCH) or dodecane exhibit a broader, blue-shifted Q band with a maximum at $\lambda = 520$ nm ($\varepsilon = 38.000\ \text{M}^{-1}\text{cm}^{-1}$; Figure 2a,b and Figure S2).[16] Similarly, molecules **1α** and **1β** in dioxane show a strong emission band, typical of SubPc monomers, with emission maxima at $\lambda = 590$ nm. In contrast, MCH solutions of **1α/β** are virtually non-emissive (Figure 2c,d and S2). Both the presence of the small axial fluorine atom and the peripheral amide substituents are required for these spectroscopic changes in apolar solvents, as none of compounds **2**, **3**, and **4** display such features. Thus, we attribute the spectral features measured in apolar solvents to the formation of head-to-tail columnar supramolecular polymers of **1α/β**, as depicted in Figure 1a. CD spectroscopy was consistent with this hypothesis (Figure 2e,f). Compounds **1α** or **1β** in the monomer state exhibit a mirror-imaged CD signal centered at $\lambda = 578$ nm, negative for **1α** and positive for **1β**.[14] In MCH, in contrast, *M*- and *P*-helical homochiral stacks are formed that show a Cotton effect with a zero-crossing at the $\lambda = 520$ nm aggregate absorption maximum wavelength. Hydrogen bonding between the exocyclic amide groups was confirmed by ^{1}H NMR and FTIR spectroscopy.

The dissociation of **1α/β** stacks can be monitored by spectroscopy as a function of sample concentration, temperature, or solvent composition. Figures 2a, c, and e show the absorption, emission, and CD changes, respectively, occurring in the transition from the supramolecular polymer to the monomer as the volume fraction of dioxane (χ_d) in MCH:dioxane mixtures is increased. Increasing the sample temperature of MCH solutions results in similar changes (Figure 2b, d, and f). Consistent with a supramolecular polymerization process, the degree of aggregation (α) decreases at high temperatures and at low concentrations (Figure S3). The self-assembly mechanism has been analyzed by fitting the

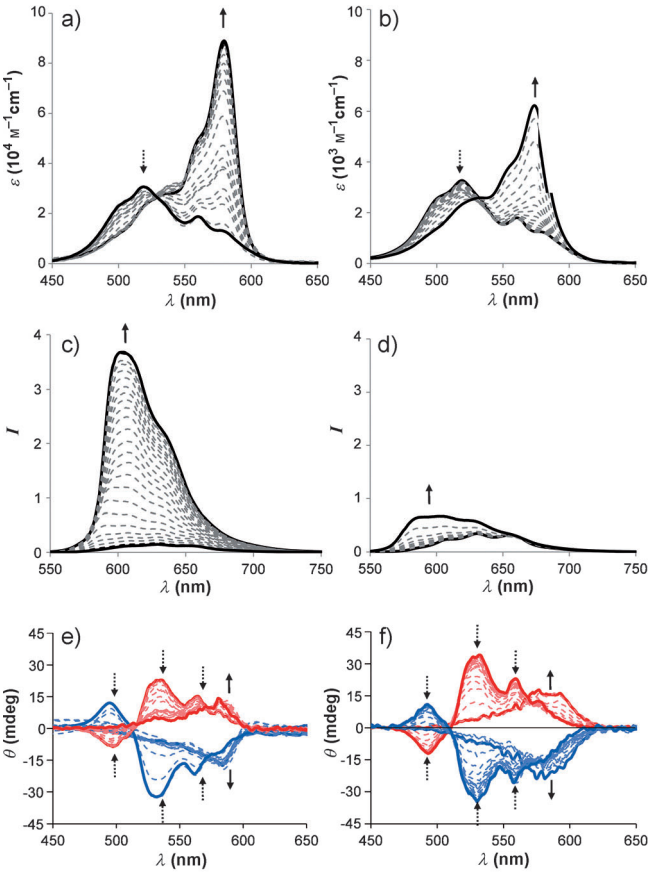

Figure 2. Q-band a, b) UV/Vis absorption, c, d) emission, and e, f) circular dichroism spectral changes of SubPc **1α** and **1β**. Changes are recorded as a function of a, c, e) the volume fraction of dioxane (χ_d) in MCH:dioxane mixtures (from $\chi_d = 0$–0.35; $[\mathbf{1\alpha}] = [\mathbf{1\beta}] = 5.0\times10^{-5}$ M), or b, d, f) the temperature ($T = 368$–268 K; $[\mathbf{1\alpha}] = [\mathbf{1\beta}] = 3.9\times10^{-6}$ M) in MCH solutions. Arrows indicate the trends with increasing χ_d or *T* values, respectively.

non-sigmoidal cooling curves, calculated from the UV/Vis absorption extinction coefficient at $\lambda = 576$ nm, to the cooperative nucleation–elongation model developed by Meijer and ten Eikelder and co-workers (Figure S4).[17] This model assumes that that after an unfavourable nucleation process, the system can abruptly elongate yielding extended supramolecular polymeric species. The data fitted reasonably well to a dimeric nucleus that then grows by successive SubPc stacking.[18] Applying the model to **1α/β** in MCH, we obtained the main thermodynamic parameters, both for the nucleation: $\Delta H°_{\text{nucl}} = -11.7 \pm 1.3\ \text{kJ mol}^{-1}$, and $K_{\text{nucl}} = 7.1\times10^3\ \text{M}^{-1}$, as well as for the elongation process: $\Delta H°_e = -56.1 \pm 3.4\ \text{kJ mol}^{-1}$, $\Delta S° = -55.0 \pm 2.8\ \text{J mol}^{-1}\text{K}$, $K_e = 4.2\times10^5\ \text{M}^{-1}$, and $T_e = 344.9 \pm 1.1$ K (where K_{nucl} and K_e refer to the equilibrium constants for nucleation and elongation, respectively). The degree of cooperativity in the self-assembly process was calculated at $\sigma = 0.017$.[15,16] These values agree reasonably well with those reported for other hydrogen-bonded polymers obtained from C_3-symmetric monomers. Our entropic term is, however, relatively small, which may reflect the high structural rigidity of our SubPc monomers.[18b]

The formation of supramolecular polymeric stacks of SubPcs **1α**/**β** was confirmed by scanning probe and electron microscopies. MCH solutions were dropcast onto highly oriented pyrolitic graphite (HOPG) and the surface was imaged by AFM after solvent evaporation. As shown in Figure 3a, long fibrillar objects were observed on the surface

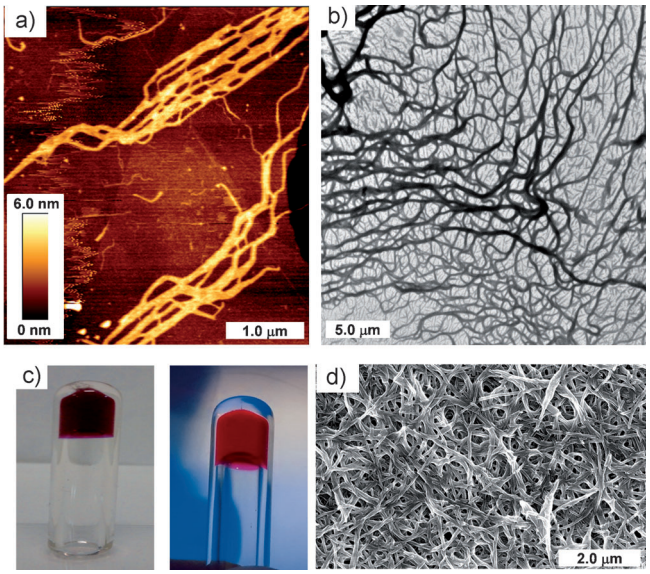

Figure 3. a) AFM height image of **1** dropcast onto HOPG ([**1**] = 3.2×10^{-6} M in MCH). b) TEM image of a negatively stained solution of **1** in MCH on a carbon-coated copper grid. c) Dodecane gels under no (left) or $\lambda = 365$ nm (right) UV irradiation. d) SEM image of the corresponding xerogel.

whose average height match those of single SubPc fibers (2.5 nm in diameter) and fiber bundles (5–6 nm), likely formed by bundling of two or three individual fibers. The high propensity of these fibers to bundle may be the reason why we could not observe helical structures. TEM analysis (Figure 3b) also showed the formation of bundled fibers in MCH or dodecane. Additionally, SubPc **1** formed stable red–magenta-colored gels in dodecane at a concentration of 4.2 mg mL^{-1}, whose fluorescence emission is quenched with respect to non-aggregated solutions in dioxane (Figure 3c). SEM images of the xerogel (Figure 3d), prepared by vacuum-drying the dodecane gels, revealed an extended and interconnected fibrous network.

Intrigued by these unique non-centrosymmetric homochiral assemblies, quantum-chemical calculations were carried out to gain further insight into the structural features of the head-to-tail stacks of **1α**/**β** at the molecular scale. We took **1β** as the model enantiomer, but the analysis performed hereafter can be equally applied to **1α**. Prior to optimizing a columnar structure, we examined the diverse conformational possibilities for the H-bonding association between amides. In **1α**/**β** there are four types of amide conformations, depending on the C-C-N-H dihedral angle formed between this group and the isoindole ring (Figure 4a). *Syn-in* and *anti-out* conformations are complementary and lead to left-handed (*M*) helices, whereas *syn-out* and *anti-in* conformations result in right-handed (*P*) helices (Figure S5). To

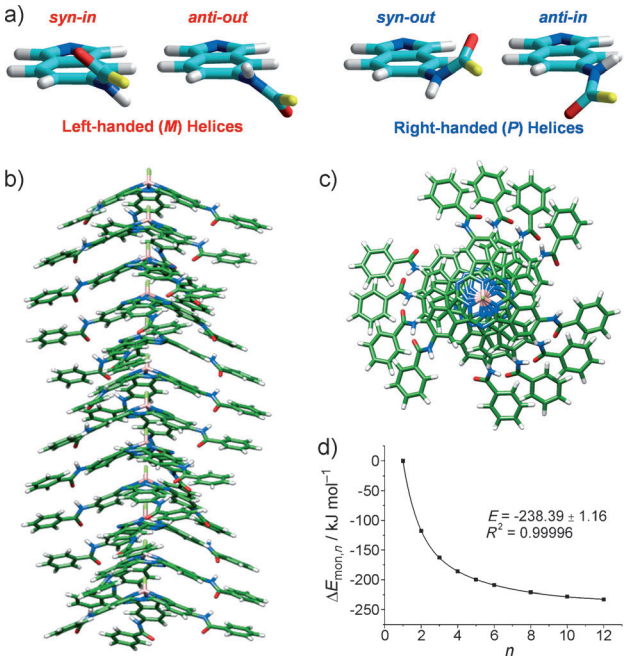

Figure 4. a) Amide conformations that lead to triple intermolecular hydrogen bonding in the **1β** helical stacks. *Syn* and *anti* orientations are defined as depending on whether the amide carbonyl dipole is aligned parallel or antiparallel, respectively, to the axial B–F bond. *In* and *out* orientations describe the position of the carbonyl oxygen (red atom) with respect to the isoindole ring. b) Side and c) top views of *P*-helical *all-anti-in* head-to-tail arrangement of **1β** stacks calculated by DFT. Dodecyl chains have been replaced with hydrogen for calculations. d) Stabilization energy per monomer unit ($\Delta E_{mon,n}$) calculated at the at ωB97X-D/cc-pVTZ level as the number of monomers (*n*) in the *all-anti-in* aggregate increases. Energy values are fitted to a biexponential decay function (solid line). Atom colors in (a, b, c): O = red; N = dark blue; H = white; simplified R group in (a) = yellow; C = green (in (b) and (c); C = turquoise in (a)).

identify which conformation is energetically favored, we considered three different issues: intermolecular interactions, the net dipole moment, and chiral helicity.

First, head-to-tail **1β** dimers were built and fully optimized at the B97-D/6-31G** level (Figure S6–S8). Right-handed *syn-out* and *anti-in* conformations lead to *P*-helical dimers stabilized by both π–π and H-bonding interactions between the three amide groups (see Figure S8). A significantly different situation is noted however for *M*-helical *syn-in* and *anti-out* conformations, for which theoretical models reveal that the amide groups cannot adopt an optimal orientation for H-bond formation and the dimers are, as a result, considerably destabilized.[15] Further comparison between *syn-out* and *anti-in* dimers (Figure S9) showed that although both dimers present similar structural parameters, the *anti-in* arrangement is computed 7.8 kcal mol^{-1} more stable than the *syn-out* configuration.

To explain this energy difference we then considered discrete interactions between dipoles. As the stack grows, a global dipole is generated along the *z* axis that feeds from two main contributions: a) the axial B–F bond, which leads to a rigid dipole that increases with stack length,[7h] and b) the *z*-

component of the amide carbonyl dipole, which can change orientation in order to add (*syn*) or subtract (*anti*) to the B–F dipole.[5] A vacuum environment (in which theoretical calculations were carried out) or solvents with low dielectric constants (such as MCH or dodecane) are not suited to stabilize polar structures. Thus we reasoned that the non-centrosymmetric stacks of **1α**/**β** must grow with a minimum global dipole moment, which may be achieved by participation of *anti* conformations. Calculations show that columnar aggregates having the three amides in the *anti-in* conformation, that is, their *z*-component dipoles opposing the B–F dipole, have minimum net dipole moments (Figure S12).

Finally, the theoretical CD spectrum was computed for both the monomer and trimer species of **1β** (Figure S10). For the monomer, only one positive CD signal is predicted, in agreement with the experimental results (Figure S1). However, a more intense, blue-shifted, negative-to-positive CD signal is predicted for the *anti-in* right-handed trimer of **1β** (Figure S10a), which also corresponds to the experimental CD spectra (Figure 2e,f) and confirms the *P* helicity of the columnar stacks formed by **1β**. The theoretical CD spectrum computed for the less stable *P*-helical *syn-out* conformation of **1β** (Figure S10b) significantly differs from the experimental data, so this conformation was again ruled out.[15] A similar analysis was made for **1α** that corroborates the formation of *all-anti-in M*-helical stacks.

In summary, theoretical calculations select the *anti-in* as the most stable configuration for the triple array of hydrogen bonds in our homochiral SubPc assemblies. This amide conformation maximizes intermolecular interactions, leads to a minimum net dipole moment in the stacking direction, and corresponds to the experimental CD spectra of the assemblies.[19] With this information in hand, **1β** *all-anti-in* columnar aggregates of increasing size (up to the dodecamer) were built up and theoretically investigated by using the long-range corrected ωB97X-D functional and the more extended triple-ζ cc-pVTZ basis set.[20] As observed in Figures 4b and c, a right-handed *anti-in* helical stacking favors the coexistence of intermolecular H-bonding, π–π stacking, and dipolar interactions. Neighboring molecules are separated by 4.12 Å and rotated by 23.0°. This torsional angle, which establishes that 16 molecules are necessary to complete one helical pitch, is dictated by the triple array of hydrogen bonds. The amide groups are twisted out the plane of the isoindole units by 36.5° to maximize the intermolecular H-bonding interactions, and give rise to NH···O intermolecular contacts of 1.93 Å. Intermolecular C···C contacts between the isoindole phenyl rings of neighboring molecules are found in the range 3.50–4.10 Å indicating that, despite the steric effect of the axial ligand, stabilizing π–π interactions are also present in these columnar arrangements. The $F^{\delta-}\cdots B^{\delta+}$ contacts between adjacent molecules are calculated to measure 2.78 Å, which are just slightly longer than twice the covalent B–F bond (1.37 Å) and significantly shorter than the sum of the van der Waals radii of boron (1.92 Å) and fluorine (1.47 Å). This evidences strong dipolar interaction between B–F dipoles along the stacks, which may account for their remarkable stability as noted in the spectroscopic studies.

Figure 4d shows the stabilization energy per monomer unit ($\Delta E_{mon,n}$) calculated for $(\mathbf{1\beta})_n$ *all-anti-in* columnar aggregates with increasing numbers of monomeric units ($n = 1$–6, 8, 10, 12). As the columnar stack grows, the H-bonding network strengthens because of the larger polarization, and the aggregate becomes more stable. It is worth noting that the asymptotic limit ($n = \infty$) is rapidly approached upon addition of 10–12 monomer units, as the increase in stabilization is relatively small with subsequent monomer additions from this point. The stabilization per monomer unit predicted for the dodecamer is $-232.9\ kJ\,mol^{-1}$, very close to that obtained from the extrapolation to $n = \infty$ ($-238.4\ kJ\,mol^{-1}$). The enhancement in $\Delta E_{mon,n}$ with increasing numbers of monomer units (n) suggests a large cooperative character for the self-association of SubPc **1**, in agreement with the experiments.

We have demonstrated for the first time the formation of non-centrosymmetric homochiral columnar SubPc assemblies through a cooperative supramolecular polymerization process driven by a combination of noncovalent interactions: H-bonding, π–π stacking, and dipolar interactions between axial dipolar B–F bonds. Future work will focus on exploiting the axial dipole moments generated in these assemblies to produce electric-field-responsive polar materials that may exhibit ferroelectricity.

Received: November 20, 2014
Published online: January 19, 2015

Keywords: homochiral aggregates · porphyrinoids · self-assembly · subphthalocyanine · supramolecular polymerization

[1] S. Laschat, A. Baro, N. Steinke, F. Giesselmann, C. Hägele, G. Scalia, R. Judele, E. Kapatsina, S. Sauer, A. Schreivogel, M. Tosoni, *Angew. Chem. Int. Ed.* **2007**, *46*, 4832–4887; *Angew. Chem.* **2007**, *119*, 4916–4973.

[2] a) S. Shimizu, A. Miura, S. Khene, T. Nyokong, N. Kobayashi, *J. Am. Chem. Soc.* **2011**, *133*, 17322–17328; b) G. Markopoulos, L. Henneicke, J. Shen, Y. Okamoto, P. G. Jones, H. Hopf, *Angew. Chem. Int. Ed.* **2012**, *51*, 12884–12887; *Angew. Chem.* **2012**, *124*, 13057–13060.

[3] K. Sato, Y. Itoh, T. Aida, *Chem. Sci.* **2014**, *5*, 136–140.

[4] A. R. A. Palmans, E. W. Meijer, *Angew. Chem. Int. Ed.* **2007**, *46*, 8948–8968; *Angew. Chem.* **2007**, *119*, 9106–9126.

[5] a) D. Miyajima, F. Araoka, H. Takezoe, J. Kim, K. Kato, M. Takata, T. Aida, *Angew. Chem. Int. Ed.* **2011**, *50*, 7865–7869; *Angew. Chem.* **2011**, *123*, 8011–8015; b) D. Miyajima, F. Araoka, H. Takezoe, J. Kim, K. Kato, M. Takata, T. Aida, *Science* **2012**, *336*, 209–213.

[6] T. Amaya, S. Seki, T. Moriuchi, K. Nakamoto, T. Nakata, H. Sakane, A. Saeki, S. Tagawa, T. Hirao, *J. Am. Chem. Soc.* **2009**, *131*, 408–409.

[7] The head-to-tail columnar stacking of cone- or bowl-shaped molecules has been, however, demonstrated in crystal and liquid-crystal structures. See: a) M. Sawamura, K. Kawai, Y. Matsuo, K. Kanie, T. Kato, E. Nakamura, *Nature* **2002**, *419*, 702–705; b) H. Sakurai, T. Daiko, H. Sakane, T. Amaya, T. Hirao, *J. Am. Chem. Soc.* **2005**, *127*, 11580–11581; c) S. Rodríguez-Morgade, C. G. Claessens, A. Medina, D. González-Rodríguez, E. Gutierrez-Puebla, A. Monge, I. Alkorta, J. Elguero, T. Torres, *Chem. Eur. J.* **2008**, *14*, 1342–1350; d) A. S. Filatov, E. A.

Jackson, L. T. Scott, M. A. Petrukhina, *Angew. Chem. Int. Ed.* **2009**, *48*, 8473 – 8476; *Angew. Chem.* **2009**, *121*, 8625 – 8628; e) D. Miyajima, K. Tashiro, F. Araoka, H. Takezoe, J. Kim, K. Kato, M. Takata, T. Aida, *J. Am. Chem. Soc.* **2009**, *131*, 44 – 45; f) B. M. Schmidt, S. Seki, B. Topolinski, K. Ohkubo, S. Fukuzumi, H. Sakurai, D. Lentz, *Angew. Chem. Int. Ed.* **2012**, *51*, 11385 – 11388; *Angew. Chem.* **2012**, *124*, 11548 – 11551; g) J. G. Brandenburg, S. Grimme, P. G. Jones, G. Markopoulos, G. Hopf, M. K. Cyranski, D. Kuck, *Chem. Eur. J.* **2013**, *19*, 9930 – 9338; h) J. Guilleme, J. Aragó, E. Ortí, E. Cavero, T. Sierra, J. Ortega, C. L. Folcia, J. Etxebarria, D. González-Rodríguez, T. Torres, *J. Mater. Chem.* DOI: 10.1039/c4tc02662d.

[8] a) Y.-T. Wu, J. S. Siegel, *Chem. Rev.* **2006**, *106*, 4843 – 4867; b) T. Amaya, T. Hirao, *Chem. Commun.* **2011**, *47*, 10524 – 10535.

[9] a) C. G. Claessens, D. González-Rodríguez, T. Torres, *Chem. Rev.* **2002**, *102*, 835 – 853; b) S. Shimizu, N. Kobayashi, *Chem. Commun.* **2014**, *50*, 6949 – 6966; c) C. G. Claessens, D. González-Rodríguez, M. S. Rodríguez-Morgade, A. Medina, T. Torres, *Chem. Rev.* **2014**, *114*, 2192 – 2277.

[10] S. Samdal, H. V. Volden, V. R. Ferro, J. M. García de La Vega, D. González-Rodríguez, T. Torres, *J. Phys. Chem. A* **2007**, *111*, 4542 – 4550.

[11] a) C. G. Claessens, D. González-Rodríguez, T. Torres, G. Martín, F. Agulló-López, I. Ledoux, J. Zyss, V. R. Ferro, J. M. García de La Vega, *J. Phys. Chem. B* **2005**, *109*, 3800 – 3806; b) H. Xu, X.-J. Jiang, E. Y. M. Chan, W.-P. Fong, D. K. P. Ng, *Org. Biomol. Chem.* **2007**, *5*, 3987 – 3992; c) D. González-Rodríguez, E. Carbonell, D. M. Guldi, T. Torres, *Angew. Chem. Int. Ed.* **2009**, *48*, 8032 – 8036; *Angew. Chem.* **2009**, *121*, 8176 – 8180; d) D. González-Rodríguez, E. Carbonell, G. de Miguel Rojas, C. Atienza Castellanos, D. M. Guldi, T. Torres, *J. Am. Chem. Soc.* **2010**, *132*, 16488 – 16500.

[12] a) D. González-Rodríguez, T. Torres, D. M. Guldi, J. Rivera, M. A. Herranz, L. Echegoyen, *J. Am. Chem. Soc.* **2004**, *126*, 6301 – 6313; b) D. González-Rodríguez, C. G. Claessens, T. Torres, S.-G. Liu, L. Echegoyen, N. Vila, S. Nonell, *Chem. Eur. J.* **2005**, *11*, 3881 – 3893.

[13] a) X. Tong, S. R. Forrest, *Org. Electron.* **2011**, *12*, 1822 – 1825; b) G. E. Morse, J. S. Castrucci, M. G. Helander, Z.-H. Lu, T. P. Bender, *ACS Appl. Mater. Interfaces* **2011**, *3*, 3538 – 3544; c) S. M. Menke, W. A. Luhman, R. J. Holmes, *Nat. Mater.* **2012**, *12*, 152 – 157.

[14] The structure of enantiomers **1α** and **1β** was assigned on the basis of their CD signature compared to literature data for related SubPcs (Ref. [2a]), as well as on their DFT-computed theoretical CD spectra.

[15] See the Supporting Information for further details.

[16] Data for **1β**. Racemic **1** or pure enantiomers **1α** or **1β** display identical spectroscopic features in the different solvents studied.

[17] a) A. J. Markvoort, H. M. M. ten Eikelder, P. A. J. Hilbers, T. F. A. de Greef, E. W. Meijer, *Nat. Commun.* **2011**, *2*, 509; b) H. M. M. ten Eikelder, A. J. Markvoort, T. F. A. de Greef, P. A. J. J. Hilbers, *J. Phys. Chem. B* **2012**, *116*, 5291 – 5301.

[18] a) M. J. Mayoral, C. Rest, V. Stepanenko, J. Schellheimer, R. Q. Albuquerque, G. Fernández, *J. Am. Chem. Soc.* **2013**, *135*, 2148 – 2151; b) F. García, P. A. Korevaar, A. Verlee, E. W. Meijer, A. R. A. Palmans, L. Sánchez, *Chem. Commun.* **2013**, *49*, 8674 – 8676; c) C. Rest, M. J. Mayoral, K. Fucke, J. Schellheimer, V. Stepanenko, G. Fernández, *Angew. Chem. Int. Ed.* **2014**, *53*, 700 – 705; *Angew. Chem.* **2014**, *126*, 716 – 722.

[19] N. Kobayashi, A. Muranaka, J. Mack, *Circular Dichroism and Magnetic Circular Dichroism Spectroscopy for Organic Chemists*, RSC Publishing, Cambridge, **2012**.

[20] The monomer used to build up the oligomers and the relative disposition of the adjacent molecules along the stack were obtained from the ωB97X-D/6-31G** fully optimized structure of the heptamer (see the Supporting information for full computational details).

